

Localization of charge carriers in layered crystals Me_xTiSe_2 (Me = Cr, Mn, Cu) studied by the resonant photoemission

Y. M. Yarmoshenko,¹ A. S. Shkvarin,¹ M. V. Yablonskikh,² A. I. Merentsov,^{1,3}
 and A. N. Titov^{1,3}

¹*Institute of Metal Physics, Russian Academy of Sciences-Ural Division, 620990 Ekaterinburg, Russia*

²*Sincrotrone Trieste SCpA, Basovizza I-34012, Italy*

³*Ural Federal University, 620083 Ekaterinburg, Russia*

(Received 23 July 2013; accepted 13 September 2013; published online 1 October 2013)

The probability of charge transfer in layered titanium diselenide between monolayers containing Cr, Mn, and Cu with different concentrations and host lattice TiSe_2 is estimated according to the resonant photoemission data. For this purpose, the Raman-Auger contributions and narrow bands just below the Fermi energy were separated in the valence band spectra. These contributions provide the information about charge transfer. It is shown that the localization of the 3d electrons is typical for Cr and Cu atoms and strongly depends on their concentration. In Mn_xTiSe_2 , Mn 3d electrons are delocalized and the probability of the charge transfer is the greatest as compared with other compounds under investigation. © 2013 AIP Publishing LLC.

[<http://dx.doi.org/10.1063/1.4824060>]

I. INTRODUCTION

TiSe_2 is a member of the big family of layered transition-metal dichalcogenides with 1T-CdI_2 structure and the quasi-two-dimensional character of electronic properties. TiSe_2 consists of complex chalcogen-metal-chalcogen layers (slabs) with strong ionic bond inside the slabs and van der Waals bond between the slabs. This weak van der Waals interaction is the reason of titanium diselenide's quasi-two-dimensional properties. The physical properties of these materials depend on the character of the chemical bond between monoatomic layer of 3d metal atoms intercalated in the van der Waals gap and TiSe_2 host lattice. The strength of the chemical bond is determined by the charge state of the atoms of interest. This information is traditionally provided by the theoretical calculations of the electronic structure of clusters containing structural fragments of layered dichalcogenides¹ and the by results of measurements of photoelectron spectra of the core levels Ti 2p and Me 2p. Comparison of theoretical calculations of the charge transfer (CT) with the core level binding energy shifts often does not lead to unambiguous conclusions despite of the seeming simplicity of this approach. It is caused by the uncertainty of the spectral contributions that have different signs and origin. In the last two decades, more multipurpose photoemission methods based on the resonant excitation of core levels^{2,3} have been developed. The resonant excitation of 2p levels is often used for 3d metals. The relaxation of the excited state mainly occurs by two channels—the “spectator” and the “participant.” The “spectator” contribution describes by the resonant Raman Auger spectra (RRAS). The Auger line $L_3\text{VV}$ appears when the excitation energy is increased. The “participant” contribution describes the narrow band just below the Fermi energy (or at the maximal kinetic energy).

The concept of “small” and “large” systems, introduced in Ref. 3, is convenient in the consideration of the layered crystals. By the “small” system, one means an atom or a

molecule from the “upper layer” of the crystal under investigation. In our case, the “small” system is atomic monolayers of 3d Me in the van der Waals gap. The “large” system is a slab Se-Ti-Se (Fig. 1).

From this point of view, titanium dichalcogenides are multilayer interfaces. “Small” and “large” systems interact with each other through the spatial polarization (clouds of electrons from external shell) and charge transfer. In a first approximation, the “small” system can be considered as an isolation from the “large” and underwent a small perturbation. Charge transfer can be described as a tunneling process of the charge redistribution⁴ between “large” and “small” systems. The value of this small perturbation can be estimated quantitatively from the autoionization spectra analysis in terms of the probability of the charge transfer and the lifetime (relaxation processes) of the excited states. Therefore, the final goal of the measurements is to get the values of probability and electron's tunneling time between the “large” and “small” systems rather than an exact amount of transferred charge.

We consider two types of the interaction between “large” and “small” systems. The first type is described above charge transfer between the Me monolayer and the TiSe_2 matrix in the c -axis direction in the Me_xTiSe_2 single

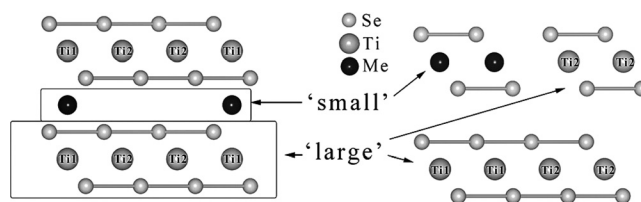


FIG. 1. Crystal structure of Me_xTiSe_2 (Me—transition metal). The “small” system—monolayer of 3d Me in the Van der Waals gap. The “large” system—Se-Ti-Se slabs. The left panel shows the structure of the intercalated system, the right panel shows the structure with substitution of Ti atoms in the host lattice by the atoms of 3d Me.

crystals (Figure 1, left panel). The second type corresponds to the interaction between Ti-Se and Cr-Se clusters in the in-plane direction in $\text{Cr}_x\text{Ti}_{1-x}\text{Se}_2$ single crystals (Figure 1, right panel). In these samples, Ti atoms are partially substituted by Cr atoms in TiSe_2 host lattice and the intercalation is absent.

The resonant photoelectron spectroscopy allows one to perform such measurements in the energy scale sufficient for the time resolution of the system's states, which are caused by the charge transfer and localization. The measurements were carried out for Me_xTiSe_2 ($\text{Me} = \text{Cr}, \text{Mn}, \text{Cu}$) compounds.

II. EXPERIMENT

Single crystals for the X-ray spectral measurements were grown by the gas transport reaction method in evacuated quartz ampoules with iodine as the gas carrier.⁵ Compounds with intercalation: $\text{Cu}_{0.07}\text{TiSe}_2$, $\text{Cu}_{0.58}\text{TiSe}_2$, $\text{Mn}_{0.1}\text{TiSe}_2$, $\text{Mn}_{0.2}\text{TiSe}_2$, $\text{Cr}_{0.19}\text{TiSe}_2$, $\text{Cr}_{0.33}\text{TiSe}_2$ and compounds with substitution of titanium by chromium: $\text{Cr}_{0.2}\text{Ti}_{0.85}\text{Se}_2$, $\text{Cr}_{0.78}\text{Ti}_{0.36}\text{Se}_2$ (for simplicity, the system with substitution will be written as “ CrSe_2 ”) were investigated. The single crystals had a shape of thin plates $\approx 2 \times 3 \text{ mm}^2$ large and $\approx 0.05 \text{ mm}$ thick. Spectroscopic measurements were performed at the standard setup BACH⁶ and CIPO⁷ beamlines of the Elettra synchrotron facility. X-ray absorption spectra (XAS) were collected in the total electron yield (TEY) mode. The samples were cleaved *in situ* in a vacuum of $3\text{--}5 \times 10^{-9}$ Torr. X-ray photoelectron spectra (XPS) of the C 1s, O 1s, and Ti 2p core levels were measured from time to time to check for a possible contamination of the surface during the measurements. The intensities of the carbon and oxygen 1s peaks in the survey spectra were extremely low, and the shape of the Ti 2p XPS remained unchanged during the measurement. The absence of titanium oxide like satellite peaks in the Ti 2p XPS ensures the negligible influence of probable oxidation of both the sample surface and the bulk material. The angle between the incident beam and the perpendicular to the basal plane of the sample was 60° . The perpendicular to the sample coincides with the c axis [001] which was aligned with the analyzer axis. Both the c axis of the sample and the polarization of the incident x-ray were in the horizontal plane. The energy resolution of the monochromator, i.e., the energy resolution of the x-ray absorption spectra was set to 0.1 eV. The photoelectron analyzer resolution was set up to 0.19 eV. The binding energy scales were calibrated according to the Fermi edge measurements of gold. The valence band spectra “at resonance” were obtained using excitation energy corresponding to the resonant excitation maximum (E_{MAX}).⁸ The valence band spectra “off-resonance” were obtained using energy $\approx E_{\text{MAX}} - 5 \text{ eV}$; the “off-resonance” energies are: 450 eV for Ti 2p-3d resonance, 560 eV for Cr 2p-3d resonance, 922 eV for Cu 2p-3d resonance, and 630 eV for Mn 2p-3d resonance.

III. RESULTS AND DISCUSSION

The spectrum of the valence bands of the compounds under investigation consists mainly of three contributions:

- Main line: the part away from the absorption edges of 3d metals containing spectrum from Se 4p and Se 4s states as a major contribution;
- Spectrum of Me 3d electrons occupying the same energy range as Se 4p state;
- The contributions of the resonant Raman Auger spectrum and a narrow band located just below the Fermi energy.

The contribution of a narrow band is directly related to the charge transfer process. The part of the Me_xTiSe_2 valence band that corresponds to Se 4s states obviously does not resonate in this region of excitation energies and its intensity is independent of the energy of excitation (as seen from Figure 2 (left panel)). Therefore, considering the Se 4s line as internal standard, one can use it to the spectral intensity normalization. We are interested in the spectral contributions of RRAS and CT.

Figure 2 (left panel) shows the primary spectra measured at the incident radiation energy in the vicinity of corresponding absorption edges of Ti. In the right panel of Figure 2, the processed spectra are shown. The processing consists of four steps: (1) background subtraction using standard algorithm;⁹ (2) normalization of spectra “at resonance” and “off-resonance” to Se 4s line ($E_B = 13.6 \text{ eV}$); (3) subtraction of the spectrum “off-resonance” from the spectrum “at resonance”; (4) normalization of the spectrum obtained at steps 1–3 to RRAS line.

Before analyzing the quantitative ratio of these contributions, let us discuss the role of the spectra's additivity associated with the crystallographically nonequivalent position of titanium and selenium atoms in Me_xTiSe_2 . We can distinguish two types of Ti: Ti1 and Ti2 (see Fig. 1) (coordinated or not coordinated by intercalated metal). The probability of filling of this octahedral position depends on the Me concentration. In fact, this observation was noted in the experimental Ti 2p spectra already in the early works.¹⁰ In the valence band spectra, the effect of additivity was not observed. It can be clearly seen in the titanium absorption spectra in Refs. 11–13 (and also in Ref. 14, where Ti $L_{2,3}$ XAS in Fe_xTiS_2 for a wide range of iron concentrations is studied). It means that the crystallographically nonequivalent titanium atoms

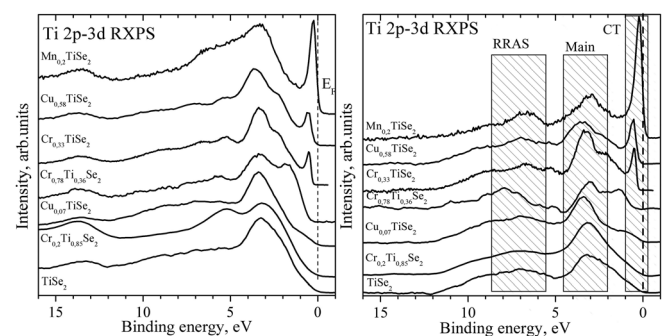


FIG. 2. Primary spectra of compounds under discussion at Ti 2p-Ti 3d resonance (left panel) and spectra after special processing (right panel). The primary spectra are normalized to the main peak with $E_B \sim 3 \text{ eV}$. All the processed spectra are normalized to the RRAS peak. Excitation energies are: $\text{TiSe}_2 - 458.3 \text{ eV}$, $\text{Cr}_{0.2}\text{Ti}_{0.85}\text{Se}_2 - 458.35 \text{ eV}$, $\text{Cu}_{0.07}\text{TiSe}_2 - 458.3 \text{ eV}$, $\text{Cr}_{0.78}\text{Ti}_{0.36}\text{Se}_2 - 458.3 \text{ eV}$, $\text{Cr}_{0.33}\text{TiSe}_2 - 457.4 \text{ eV}$, $\text{Cu}_{0.58}\text{TiSe}_2 - 458.35 \text{ eV}$, $\text{Mn}_{0.2}\text{TiSe}_2 - 456.6 \text{ eV}$.

yield the one band picture and therefore are indistinguishable in this sense.

Now on the grounds of the foregoing we can consider the spectral contributions of RRAS and CT as related to the whole crystal, but not to the separate fragments with the Ti1 and Ti2 positions. Qualitative analysis of such contributions was previously made in some papers, such as Ref. 15, devoted to the study of physisorption in system Ar/Pt (111). The lifetime of the excited by means of the photoemission $2p^53d^n$ state or its relaxation time at resonance depends on two processes: RRAS and CT. Taking into account only these two processes, we can write that $P_{CT} + P_{RRAS} = 1$, where P_{CT} is the probability of charge transfer, P_{RRAS} is the probability of the charge localization or of the formation of a bound state by means of autoionization, which is described by the RRAS spectrum. The probabilities can be obtained numerically as

$$P_{CT} = I_{CT}/(I_{CT} + I_{RRAS}), \quad P_{RRAS} = I_{RRAS}/(I_{CT} + I_{RRAS}), \quad (1)$$

where I_{CT} and I_{RRAS} are the integrated intensities of the corresponding contributions, as proposed in Ref. 3. In Figures 2(right panel) and 3, the resonant valence band spectra after special processing, as described above, are shown. CT bands just below the Fermi energy appear most clearly in Ti 2p resonance (Fig. 2) (because the titanium atoms with its almost empty 3d shell behave themselves in the host lattice like a large charge reservoir).

To define the probability more accurate, it is better to use the ratio of the corresponding peaks areas. Figure 4 shows an example of decomposition into the components and following fitting of the $Mn_{0.2}TiSe_2$ spectrum, as well as the ratios of the areas corresponding to the ‘‘Main’’ and ‘‘CT’’ peaks relative to the RRAS peak.

In the set of crystals under investigation, the probability P_{CT} , obtained from Ti 2p resonant valence band spectra, changes on the order by magnitude from $P_{CT} = 0$ in ‘‘CrSe₂’’ to $P_{CT} = 0.58$ in $Mn_{0.2}TiSe_2$ (Table I).

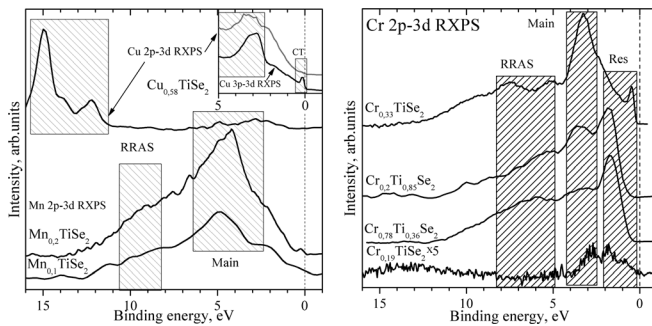


FIG. 3. The resonant Me 2p-3d spectra (Cr 2p-3d on the right panel, Cu and Mn on the left panel) after special processing. The processed spectra are normalized to RRAS peak. The intensity of the $Cr_{0.19}TiSe_2$ spectrum is not normalized to the RRAS peak because of the very low intensity of RRAS peak and is given after subtracting (step 3 of special processing) and multiplying resulting intensity on 5. Difference between Cu 2p-3d and Cu 3p-3d resonance spectra without processing is shown on inset on right panel. Excitation energies are: $Mn_{0.1}TiSe_2$ – 636 eV, $Mn_{0.2}TiSe_2$ – 636 eV, $Cu_{0.58}TiSe_2$ – 929.3 eV (Cu 2p-3d), $Cu_{0.58}TiSe_2$ – 74 eV (Cu 3p-3d), $Cr_{0.19}TiSe_2$ – 575.4 eV, $Cr_{0.2}Ti_{0.85}Se_2$ – 575.9 eV, $Cr_{0.78}Ti_{0.36}Se_2$ – 576 eV, $Cr_{0.33}TiSe_2$ – 576 eV.

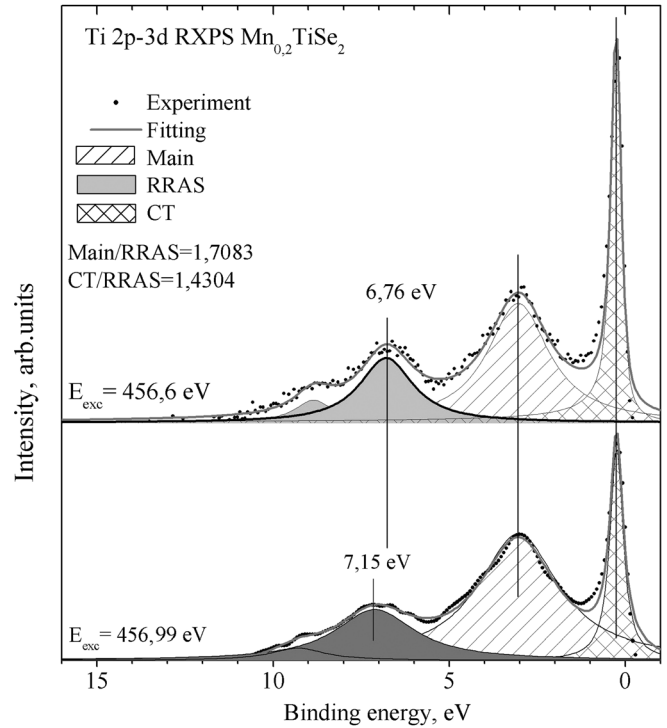


FIG. 4. An example of the spectrum decomposition to determine the contributions ratio from the different components of the spectrum. The upper spectrum corresponds to maximum resonance energy (456.6 eV), the bottom spectrum corresponds to higher energy (456.99 eV). The difference in the intensity of resonance peak (0.3 eV) and shift of RRAS peak (6.76 eV \rightarrow 7.15 eV) are clearly seen.

It confirms the previously conclusions about the absence of charge transfer in ‘‘CrSe₂’’-type crystals¹³ and in Cu_xTiSe_2 crystals with $x < 0.5$.¹² The probability P_{CT} in $Mn_{0.2}TiSe_2$ is maximal. It is shown previously that a chemical bond between Mn-atoms and host lattice in this compound is partially ionic as follows from the calculations¹⁶ and experimental data.¹¹ In $Cu_{0.58}TiSe_2$, $Cr_{0.33}TiSe_2$, and $Cr_{0.5}TiTe_2$, the charge transfer probability has an intermediate value $P_{CT} = 0.1-0.2$.

While Cr and Cu are *intercalated*, the CT contribution to Cr 2p and Cu 2p resonances is detected only in $Cr_{0.33}TiSe_2$ compound (Fig. 3, right panel). The valence bands spectra of $Cu_{0.07}TiSe_2$ and $Cu_{0.58}TiSe_2$ at Cu 2p resonance do not differ from the spectra excited out off the resonance (Raman spectrum of copper is detected). The reason is

TABLE I. The peak’s areas ratios.

Sample	RRAS/(RRAS + CT)	Res/(RRAS + CT)
$TiSe_2$	1	...
$Cu_{0.07}TiSe_2$	0.945	0.055
$Cu_{0.58}TiSe_2$	0.867	0.133
$Cr_{0.2}Ti_{0.85}Se_2$	1	...
$Cr_{0.78}Ti_{0.36}Se_2$	1	...
$Cr_{0.33}TiSe_2$	0.915	0.085
$Mn_{0.2}TiSe_2$	0.411	0.588
$TiTe_2$	0.855	0.145
$Cr_{0.5}TiTe_2$	0.844	0.154

the relatively small value of the photoionization cross section of Cu 3d electrons in this region of excitation energies. However, the CT contribution to the spectrum in $\text{Cu}_{0.58}\text{TiSe}_2$ is observed in another range of the excitation energies of Cu 3p resonance (inset on Fig. 3, left panel); here, the photoionization cross section of Cu 3d electrons is an order of magnitude greater.¹⁷ The detected effects in the resonant spectra of the examined compounds are in agreement with the Ti and Cu XAS measurements data and Cr XPS 2p lines. Ti XAS spectrum in intercalated with chromium and copper titanium diselenide do not depend on chromium and copper concentrations and coincide with the spectrum of the pristine TiSe_2 (Ref. 18) in contrast to spectrum of Mn_xTiSe_2 , which demonstrates drastically changes.¹¹ Cu XAS in Cu_xTiSe_2 ($x = 0.05\text{--}0.33$) are previously investigated.¹² While $x < 0.5$ Cu XAS are identical to that of free copper atoms. It means that in the $\text{Cu}_{0.07}\text{TiSe}_2$ there is no charge transfer between the copper atoms and the host lattice, and Cu 3d electrons are localized. In $\text{Cu}_{0.58}\text{TiSe}_2$, Cu XAS have a shape typical to the metallic copper and Cu atoms are in covalent bond with TiSe_2 . In the crystals $\text{Cr}_{0.1}\text{TiSe}_2$ and “ CrSe_2 ,” the exchange magnetic splitting of Cr 2p_{3/2} lines observed^{13,19} is caused by the exchange magnetic interaction between the spin-polarized 3d electrons of chromium with a core 2p vacancy.

IV. CONCLUSIONS

Almost all the possible cases of interaction between “small” and “large” systems inside Me-TiSe₂ are observed in the investigated crystals from the point of view of the charge transfer dynamics. In Mn_xTiSe_2 , “small” and “large” systems demonstrate strong ionic interaction; the charge transfer from the manganese to the titanium atoms is observed. In “ CrSe_2 ” and in Cu_xTiSe_2 with a low copper concentration, there is no charge transfer from one system to another, and therefore the charge localization on Cr and Cu is observed. In $\text{Cr}_{0.33}\text{TiSe}_2$ and $\text{Cu}_{0.58}\text{TiSe}_2$, the tunneling (charge transfer) between “large” and “small” systems is observed, so the interaction between “small” and “large” systems is mainly covalent.

The presented approach can be successfully applied especially for two-dimensional systems with charge transfer involving atoms of transition elements with unfilled d, f shells. The need to control the charge state of thin films arise in case of designing of interfaces or thin films during the

fitting process of components concentration to obtain the required physical properties.

ACKNOWLEDGMENTS

This work was supported by RFBR Grant No. 13-03-96032-ural and by Programm of Russian Academy of Science, Project No. 12-II-2-105. Authors are grateful for synchrotrons ELETTRA for support of experimental Project Nos. 20105305, 20100397, and 20095248, the results obtained were used in this work. We acknowledge BACH beamline staff for grating their in-house beamtime and necessary support.

¹A. N. Titov, L. N. Zelenina, T. P. Chusova, and E. G. Shkvarina, *Phys. Solid State* **54**(12), 2481–2485 (2012).

²M. Ohno, *Phys. Rev. B* **50**, 2566 (1994).

³O. Bruhwiler, N. Karis, and N. Martensson, *Rev. Mod. Phys.* **74**, 703 (2002).

⁴V. May and O. Kühn, *Charge and Energy Transfer Dynamics in Molecular Systems* (Wiley-VCH, Berlin, 2000).

⁵A. S. Shkvarin, Yu. M. Yarmoshenko, M. V. Yablonskikh, N. A. Skorikov, A. I. Merentsov, M. V. Kuznetsov, and A. N. Titov, *J. Phys. Chem. Solids* **73**, 1562 (2012).

⁶M. Zangrando, M. Finazzi, G. Paolucci, G. Comelli, B. Diviacco, R. P. Walker, D. Cocco, and F. Parmigiani, *Rev. Sci. Instrum.* **72**, 1313 (2001).

⁷A. Derossi, F. Lama, M. Piacentini, T. Prospero, and N. Zema, *Rev. Sci. Instrum.* **66**, 1718 (1995).

⁸S. Hüfner, S.-H. Yang, B. S. Mun, C. S. Fadley, J. Schäfer, E. Rotenberg, and S. D. Kevan, *Phys. Rev. B* **61**, 12582 (2000).

⁹S. Tougaard, *Phys. Rev. B* **34**, 6779 (1986).

¹⁰A. Fujimori, S. Suga, H. Negishi, and M. Inoue, *Phys. Rev. B* **38**(6), 3676 (1988).

¹¹M. V. Yablonskikh, A. S. Shkvarin, Y. M. Yarmoshenko, N. A. Skorikov, and A. N. Titov, *J. Phys.: Condens. Matter* **24**, 45504 (2012).

¹²A. S. Shkvarin, Yu. M. Yarmoshenko, N. A. Skorikov, A. A. Titov, and A. N. Titov, *J. Exp. Theor. Phys.* **114**(2), 324 (2012).

¹³A. S. Shkvarin, Yu. M. Yarmoshenko, N. A. Skorikov, A. I. Merentsov, A. N. Titov, P. A. Slepukhin, D. E. Marchenko, and M. Sperling, *J. Exp. Theor. Phys.* **112**(1), 87 (2011).

¹⁴A. Yamasaki, S. Imada, H. Utsunomiya, T. Muro, Y. Saitoh, H. Negishi, M. Sasaki, M. Inoue, and S. Suga, *Physica E* **10**, 387 (2001).

¹⁵N. Mårtensson, M. Weinelt, O. Karis, M. Magnuson, N. Wassdahl, A. Nilsson, J. Stöhr, and M. Samant, *Appl. Phys. A* **65**, 159 (1997).

¹⁶A. E. Bocquet, T. Mizokawa, T. Saitoh, H. Namatame, and A. Fujimori, *Phys. Rev. B* **46**, 3771 (1992).

¹⁷J. J. Yeh and I. Lindau, “Atomic subshell photoionization cross sections and asymmetry parameters: $1 < Z < 103$,” *At. Data Nucl. Data Tables* **32**, 1 (1985).

¹⁸A. S. Shkvarin, Yu. M. Yarmoshenko, N. A. Skorikov, M. V. Yablonskikh, A. I. Merentsov, E. G. Shkvarina, and A. N. Titov, *JETP* **115**, 798 (2012).

¹⁹A. N. Titov, A. V. Kuranov, V. G. Pleschev, Yu. M. Yarmoshenko, M. V. Yablonskikh, A. V. Postnikov, S. Plogmann, M. Neumann, A. V. Ezhov, and E. Z. Kurmaev, *Phys. Rev. B* **63**, 035106 (2001).

Journal of Applied Physics is copyrighted by the American Institute of Physics (AIP).
Redistribution of journal material is subject to the AIP online journal license and/or AIP
copyright. For more information, see <http://ojps.aip.org/japo/japcr/jsp>